Microbial Cell Factories

RESEARCH

Open Access

Highly selective whole-cell 25-hydroxyvitamin D_3 synthesis using molybdenum-dependent C25-steroid dehydrogenase and cyclodextrin recycling

Dennis Kosian[1†], Max Willistein[1†], Ralf Weßbecher[1], Constantin Eggers[1], Oliver May[2] and Matthias Boll[1*]

Abstract

Background The global prevalence of vitamin D (VitD) deficiency associated with numerous acute and chronic diseases has led to strategies to improve the VitD status through dietary intake of VitD-fortified foods and VitD supplementation. In this context, the circulating form of $VitD_3$ (cholecalciferol) in the human body, 25-hydroxy-$VitD_3$ (calcifediol, 25OH$VitD_3$), has a much higher efficacy in improving the VitD status, which has motivated researchers to develop methods for its effective and sustainable synthesis. Conventional monooxygenase-/peroxygenase-based biocatalytic platforms for the conversion of $VitD_3$ to value-added 25OH$VitD_3$ are generally limited by a low selectivity and yield, costly reliance on cyclodextrins and electron donor systems, or by the use of toxic co-substrates.

Results In this study, we used a whole-cell approach for biocatalytic 25OH$VitD_3$ synthesis, in which a molybdenum-dependent steroid C25 dehydrogenase was produced in the denitrifying bacterium *Thauera aromatica* under semi-aerobic conditions, where the activity of the enzyme remained stable. This enzyme uses water as a highly selective $VitD_3$ hydroxylating agent and is independent of an electron donor system. High density suspensions of resting cells producing steroid C25 dehydrogenase catalysed the conversion of $VitD_3$ to 25OH$VitD_3$ using either O_2 via the endogenous respiratory chain or externally added ferricyanide as low cost electron acceptor. The maximum 25OH$VitD_3$ titer achieved was 1.85 g L^{-1} within 50 h with a yield of 99%, which is 2.2 times higher than the highest reported value obtained with previous biocatalytic systems. In addition, we developed a simple method for the recycling of the costly $VitD_3$ solubiliser cyclodextrin, which could be reused for 10 reaction cycles without a significant loss of quality or quantity.

Conclusions The established steroid C25 dehydrogenase-based whole-cell system for the value-adding conversion of $VitD_3$ to 25OH$VitD_3$ offers a number of advantages in comparison to conventional oxygenase-/peroxygenase-based systems including its high selectivity, independence from an electron donor system, and the higher product titer and

†Dennis Kosian and Max Willistein are co-first author.

*Correspondence:
Matthias Boll
matthias.boll@biologie.uni-freiburg.de

Full list of author information is available at the end of the article

yield. Together with the established cyclodextrin recycling procedure, the established system provides an attractive platform for large-scale 25OHVitD$_3$ synthesis.

Keywords Vitamin D$_3$, 25-hydroxyvitamin D$_3$, Calcifediol, Calcitriol, Whole-cell biocatalysis, *Thauera aromatica*, Molybdenum-dependent hydroxylase, Steroid C25 hydroxylase, Cyclodextrin

Background

Vitamin D (VitD) is well known for its role in calcium and phosphate homeostasis in the human body, and a deficiency of the prohormone is primarily associated with skeletal diseases such as rickets [1]. There is now growing evidence linking VitD deficiency to cardiovascular disease, some cancers, neurological disorders, autoimmune diseases (e.g., multiple sclerosis, type 2 diabetes) and pulmonary diseases [2–4]. Recent studies have investigated the role of VitD in the context of the COVID-19 pandemic and have shown a strong correlation between low serum levels of VitD and the risk for and severity of COVID-19 infections [5, 6].

There are two forms of VitD: the VitD$_2$, found in UV-irradiated fungi or yeast, and the VitD$_3$ (cholecalciferol). The latter is synthesised in the human skin from endogenous 7-dehydrocholesterol after exposure to solar UV-B radiation to preVitD$_3$ followed by thermal isomerisation (Fig. 1A). In the liver, several cytochrome P450 enzymes (CYPs) hydroxylate VitD$_3$ to 25-hydroxy-VitD$_3$ (calcifediol, 25OHVitD$_3$), the clinically relevant, circulating form of VitD$_3$ (Fig. 1B). Finally, the active hormone calcitriol (1α,25(OH)$_2$VitD$_3$) is formed by a second CYP-dependent hydroxylation in the kidneys [2, 3].

There is a global prevalence of VitD deficiency, which has been associated with numerous acute and chronic diseases [2, 3]. The level of physiological 25OHVitD serves as an indicator of VitD deficiency, with serum concentrations below 20 μg L^{-1} (50 nmol L^{-1}) representing a threshold. Using this definition, around 40% of the European population is estimated to be VitD deficient. Strategies to improve the VitD status include dietary intake of VitD-fortified foods and supplementation [2]. Supplementation with 25OHVitD$_3$ has a number of advantages in comparison to VitD$_3$/VitD$_2$: (i) serum 25OHVitD$_3$ levels are increased more rapidly; (ii) 25OHVitD$_3$ has a linear dose-response curve; (iii) there is no dependence on liver CYPs, which is beneficial in patients with impaired hepatic function; (iv) the significantly higher water solubility of 25OHVitD$_3$ reduces its accumulation in adipose tissue and improves its uptake in patients with malabsorption [7–10]. In summary, 25OHVitD$_3$ is considered to be 3- to 6-fold more potent than VitD$_3$/VitD$_2$, which is particularly beneficial when an immediate increase in serum 25OHVitD$_3$ is required.

Due to the high efficiency of 25OHVitD$_3$ supplements in improving human VitD status, there is a high demand for effective methods to synthesise it from readily available precursors. This demand is further increased by the

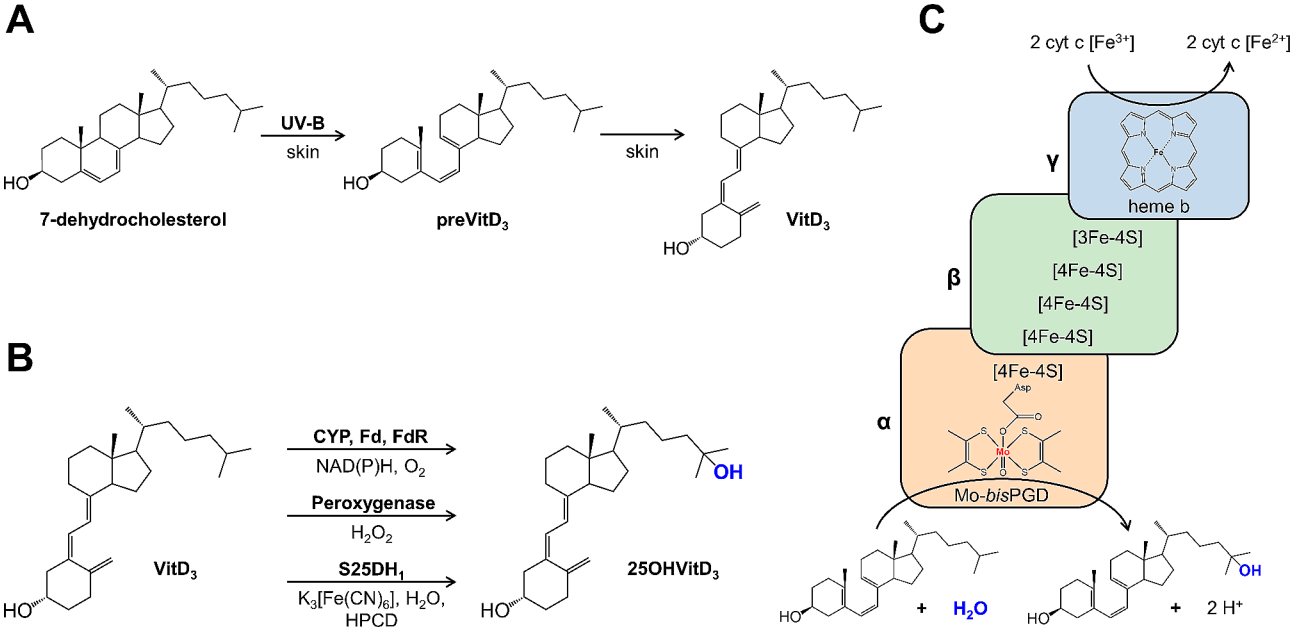

Fig. 1 Synthesis of VitD$_3$ in the human skin (**A**), hydroxylation to 25OHVitD$_3$ by different enzymes (**B**), subunit composition and reaction catalysed by S25DH$_1$ from *Sterolibacterium denitrificans* (**C**)

use of 25OHVitD$_3$ as effective feed additive for poultry or pig nutrition [11–13]. The chemical synthesis of 25OHVitD$_3$ from steroid precursors, e.g. produced in yeast, still plays an important role in industrial processes and proceeds via 25-OH-7-dehydrocholesterol followed by UV irradiation and thermal isomerization to the product [14, 15]. However, the rather low yields and selectivity, especially with respect to the hydroxylation at C25, have motivated researchers to explore one-step enzymatic systems that directly convert VitD$_3$ to the value-added 25OHVitD$_3$. Over the past two decades, a number of studies have evaluated numerous CYPs from vertebrate liver, fungi or bacteria for the O_2-dependent hydroxylation of VitD$_3$ to 25OHVitD$_3$ ([16], Table 1 and references therein, Fig. 1B). Since CYPs consume the electron donor NAD(P)H stoichiometrically, the costly regeneration of NAD(P)H can be facilitated by using whole-cell systems expressing CYPs.

To date, the highest titer of 25OHVitD$_3$ synthesised from VitD$_3$ via a whole-cell system involving CYPs is 830 mg L^{-1} after 60 h with a yield of 42%, as reported for *Bacillus cereus* zju 4-2 [17] (Table 1). A higher yield (74.4%) and productivity (287 mg L^{-1} h^{-1}) has been reported for a recombinant *Rhodococcus erythropolis* expressing a CYP that converts VitD$_3$ to 25OHVitD$_3$ [18]. Besides the problem of incomplete substrate conversion, a major disadvantage of CYP enzymes is their rather low specificity, often leading to the formation of undesired by-products requiring expensive HPLC-based purification protocols. In particular, the formation of the highly potent hormone calcitriol after a second hydroxylation at C1 is problematic. As an alternative, fungal peroxygenases have been used for the hydroxylation of VitD$_3$ to 25OHVitD$_3$, using H_2O_2 instead of O_2+NAD(P)H as co-substrate [19, 20] (Fig. 1B). However, peroxygenase-dependent systems are typically used in vitro due to their toxic co-substrate.

Steroid C25 dehydrogenases (S25DHs) have been identified in facultatively anaerobic bacteria that use side-chain containing steroids as a carbon and energy source under denitrifying conditions, and hydroxylate their substrate to C25 tertiary alcohols [25, 26]. These enzymes with moderate oxygen sensitivity (50% loss of activity in crude extracts after 24 h) belong to the dimethylsulfoxide (DMSO) reductase family of molybdenum cofactor (Moco) containing enzymes, are composed of three subunits, and use water as hydroxylating agent (Fig. 1C). A periplasmic S25DH (designated S25DH$_1$) has originally been isolated from the Gram-negative β-proteobacterium *Sterolibacterium denitrificans* and most likely uses cytochrome c as in vivo electron acceptor, which can be replaced by the artificial ferricyanide ($K_3[Fe(CN)_6]$) in vitro [25]. Catalysis takes place at Moco (molybdo-*bis*-pyranopterin guanine dinucleotide, Mo-*bis*PGD) bound to the α-subunit, while the β- (FeS cluster cofactors), and γ-subunits (heme b cofactor) are involved in electron transfer from the substrate to the external acceptor. A fourth gene product (δ-'subunit') serves as an essential chaperone for proper folding and cofactor insertion. The proposed mechanism of S25DHs involves hydride abstraction from tertiary C25 to the oxidised Mo(VI)=O yielding Mo(IV)–OH and a carbocation intermediate, followed by the transfer of the hydroxyl group back to C25 of the substrate [27]. In addition to the natural substrate, cholest-4-en-3-one, S25DH$_1$ from *S. denitrificans* converts VitD$_3$ to 25OHVitD$_3$ with an apparent selectivity of 100% in the presence of 2-hydroxypropyl-β-cyclodextrin (HPCD) and $K_3[Fe(CN)_6]$ as acceptor [28]. Recently, we established a heterologous production platform for the three structural subunits and the chaperone in the denitrifying β-proteobacterium *Thauera aromatica* K172. Heterologous overproduction of the S25DH$_1$ was achieved using an isopropyl β-D-1-thiogalactopyranoside (IPTG) induced *tac* promotor in the presence of gentamycin, resulting in a 6.5-fold higher specific activity in the soluble cell extract of. *T. aromatica* than in that of the wild type reaching 2.9 nmol min^{-1} (mg protein)$^{-1}$ [29].

Table 1 Comparison of selected whole-cell based production systems of 25OHVitD$_3$

Organism	Enzyme	VitD$_3$ (mg L^{-1})	Additives	25OHVitD$_3$ (mg L^{-1})	Time	Ref.
Escherichia coli BL21 (DE3)	recombinant CYP105A1	100	dimethylsulfoxid, 1% (v/v)	2.5	24 h	[21]
Kutzneria albida	CYP	500	HPCD, 1% (w/v)	70.4	48 h	[22]
Bacillus megaterium	recombinant CYP109A2 (T103A mutant)	577	HPCD, 2.25% (w/v) saponin, 0.0825% (w/v)	282.7	48 h	[23]
Pseudonocardia sp. KCTC 1029BP	n.d.	600	ethanol, 0.2% (v/v) HPCD, 0.1% (w/v)	356	120 h	[24]
Rhodococcus erythropolis	recombinant CYP (T107A mutant)	769	partially methylated β-cyclodextrin, 1.5% (w/v)	573	2 h	[18]
Bacillus cereus zju 4-2	n.d.	2000	propylene glycol, 9% (v/v) ethanol, 1% (v/v)	830	60 h	[17]
Thauera aromatica K172	recombinant S25DH$_1$	1780	HPCD, 12.5% (w/v) ethanol, 5% (v/v)	1850	50 h	this work

Based on the established heterologous production platform for S25DHs in *T. aromatica*, we aimed to establish a whole-cell platform for the specific conversion of $VitD_3$ to 25OHVitD$_3$. Using resting *T. aromatica* cells expressing the genes encoding $S25DH_1$ and the chaperone, we achieved a product titer 2.2-fold higher than the highest reported for CYP-dependent whole-cell systems, with a selectivity > 99% and a substrate conversion > 99%. $S25DH_1$ was surprisingly oxygen tolerant in whole cells, allowing $VitD_3$ hydroxylation to be linked to the endogenous aerobic respiratory chain. Finally, an efficient procedure for HPCD recycling was established which is essential for the implementation of the whole-cell system for potential applications.

Methods

Cultivation of $S25DH_1$-producing *T. aromatica* K172

Cultivation was performed at 30 °C under fully aerobic, fully anaerobic or semi-aerobic conditions (static bottle with no active oxygen removal) in mineral salt medium at a 1 or 2 L scale as described [30]. Sodium acetate (15 mM) served as electron donor and carbon source, $NaNO_3$ (15 mM) or O_2 as electron acceptors. The pH was adjusted to 8.0. Gentamycin was added to a final concentration of 50 µg mL^{-1}. Supplementation with vitamins (VL-7 stock solution), trace elements (SL-10 stock solution) and $MgSO_4$/$CaCl_2$ stock solutions was as described [30].

Growth was monitored by optical density measurements at 578 nm ($OD_{578\ nm}$). Nitrate concentration (Quantofix nitrate/nitrite II, Macherey-Nagel, Düren, Germany) and pH (pH-Fix 4.5–10, Roth, Karlsruhe, Germany) were determined. The medium was supplemented with sodium acetate/acetic acid (depending on pH) and/or sodium nitrate in 15 mM increments. Induction of $S25DH_1$ production was achieved with 1 mM isopropyl β-D-1-thiogalactopyranoside (IPTG) at $OD_{578\ nm} \approx 0.8$ during exponential growth. When the cultures reached the stationary growth phase, the medium was no more supplemented, and the cultures were stored for up to three weeks at 30 °C or 4 °C.

Determination of dissolved dioxygen

The concentration of dissolved oxygen in aqueous solutions was determined by non-invasive optical detection using SP-Pst3-D5 sensor spots (PreSens, Regensburg, Germany) immersed in the solution and a Fibox 4 trace oxygen meter (PreSens).

Fluorescence microscopy of cell suspensions

A commercially available LIVE/DEAD™ BacLight™ Bacterial Viability Kit (Thermo Fisher Scientific, Waltham, USA) was used to investigate living/dead cells. *T. aromatica* cells were diluted to $OD_{578\ nm} = 1.0$ in dH_2O. The cell suspension (10 µL) was mixed with 10 µL of a staining solution (SYTO 9/ propidium iodide 1:1 [v/v]), incubated for 15 min at room temperature in the dark and analysed by fluorescence microscopy (Axio Imager.M2, Carl Zeiss, Oberkochen, Germany). GFP and dsRed filters were used for the LIVE/DEAD staining analysis at a 100x magnification.

$VitD_3$ conversion by whole cells

If not otherwise stated, $VitD_3$ conversion assays were usually carried out in the 250 or 500 µL scale in Eppendorf tubes. Assay mixtures contained 0–10% (w/v) HPCD, 0.5 mM $VitD_3$ (from a stock solution prepared in isopropanol), electron acceptors (0–10 mM $K_3[Fe(CN)_6]$, 2 mM $NaNO_3$ or O_2 [shaking at 500 rpm using an Eppendorf ThermoMixer®]), $S25DH_1$-producing *T. aromatica* cell suspensions at $OD_{578\ nm}$ 10–100 and a phosphate-buffered medium (5 mM NaH_2PO_4, 32 mM K_2HPO_4, 10 mM NH_4Cl at pH 8.0). The densities of *T. aromatica* cell suspensions were adjusted by centrifugation in 50 mL conical tubes (6000 rpm, 4 °C, 20 min, Eppendorf 5804R centrifuge, Rotor S-4-72) and by resuspension in the required volume of phosphate-buffered medium. For conversion under anaerobic conditions, all steps were carried out with anaerobic buffers and solutions in a forming gas atmosphere (N_2/H_2, 95:5). $VitD_3$ conversion assays were carried out for up to 24 h and sampled regularly by transferring an aliquot of the reaction mix (20 µL) into a fourfold volume excess of isopropanol (80 µL) to precipitate enzymes and cells. Product formation was detected by ultra-performance liquid chromatography (UPLC) measurements.

For whole cell conversion in the 100 mL scale, a premixed, saturated $VitD_3$ solution (≈ 9.5 mM) was mixed in a 1:1 ratio (v/v) with a cell suspension at $OD_{578\ nm} = 200$ (total reaction volume: 100 mL) and incubated at 30 °C for up to 50 h. The resulting reaction mix contained 4.63 mM of dissolved $VitD_3$ in the presence of 12.5% (w/v) HPCD and 5% (v/v) ethanol. At the beginning and after 2 h, 4 h, 22 h and 28 h, 10 mM $K_3[Fe(CN)_6]$ were added to result in a final concentration of 50 mM. The experiment was carried out for 50 h under anoxic conditions to ensure stability of the whole-cell catalyst. Samples were taken at defined time points and analysed by UPLC.

$VitD_3$ conversion by cell free extracts

A cell suspension with $OD_{578\ nm} = 200$ was disrupted after addition of DNase I (Applichem, Darmstadt, Germany) by single passage through a French pressure cell (1100 psi, SLM Aminco) to prepare cell free extracts. Protein content was determined by Bradford [31], and the final protein concentration of the diluted extract in the reaction mixture (100 µL) was 2.8 mg mL^{-1}. The setup for the $VitD_3$ conversion including sampling procedure was as

described for whole cells with 10% (w/v) HPCD, 10 mM $K_3[Fe(CN)_6]$ and 0.5 mM $VitD_3$.

Preparation of premixed aqueous solutions saturated with $VitD_3$

A solution of 50% (w/v) HPCD in ddH_2O was prepared and mixed with the required volume of 100–200 mM $VitD_3$ stock solution in ethanol to obtain a final concentration of 10–20 mM of $VitD_3$ under constant stirring. The mixture was diluted with phosphate-buffered medium to the desired final volume. Approximately 50% of the added $VitD_3$ precipitated and was removed by filtration (0.2 µm filter) to give a clear solution. Typical concentrations of 6–10 mM dissolved $VitD_3$ (as determined by UPLC analysis) were obtained in the presence of 20–25% (w/v) HPCD and 5–10% (v/v) ethanol as co-solvent.

Determination of malate dehydrogenase activity

Malate dehydrogenase activity was determined in cell free extracts and whole cells as an indicator of membrane integrity. NADH and oxaloacetate (250 µM, each) served as substrates in a 0.1 M potassium phosphate buffered (pH 7.4) environment (total volume: 0.5 mL). NADH oxidation was monitored time-dependently at 340 nm ($\varepsilon_{340\ nm}$=6.22 mM^{-1} cm^{-1}) and 30 °C using a UV-1900i UV-Vis spectrophotometer (Shimadzu Corporation, Kyoto, Japan). Samples of whole cells or cell free extracts (5% [v/v] of the reaction volume) were diluted accordingly to ensure evaluable temporal absorbance changes.

UPLC based analysis of $VitD_3$ and 25OH$VitD_3$

The conversion of $VitD_3$ to 25OH$VitD_3$ was monitored by UPLC analysis. After two centrifugation steps (20 min, RT, 14,000 rpm), samples (injection volume: 5 µL) were analysed using a Waters H-Class UPLC System (Waters, Milford, USA). Separation was achieved by reversed-phase chromatography (Waters Acquity UPLC CSH Fluoro-Phenyl column, 2.1×100 mm, 1.7 µm particle size) using an isocratic gradient of 65% acetonitrile+0.1% (v/v) formic acid for 4 min at a flow rate of 0.4 mL min^{-1} and 50 °C column temperature. Detection of steroids was achieved by absorption measurements at 260 nm using a diode array detector. For determination of absolute $VitD_3$ and 25OH$VitD_3$ concentrations, peaks at 260 nm were integrated and compared to peak areas of authentic standards (Sigma-Aldrich, Taufkirchen, Germany). The correlation between peak area and $VitD_3$/25OH$VitD_3$ concentrations was linear in a range between 10 and 500 µM. If necessary, samples were diluted in isopropanol accordingly.

Removal of cells and steroids for HPCD recycling

After conversion of $VitD_3$, cells were removed from the reaction mixture by centrifugation (6,000 rpm, 4 °C, 20 min) and the product as well as residual $VitD_3$ were extracted three times with a three-fold excess of ethyl acetate (v/v). To the remaining aqueous phase containing only HPCD and buffer components, fresh buffer was added to make up the original volume. This HPCD solution was used for the next cycle of bioconversion.

Quantitative HPCD determination

The photometric determination of HPCD was modified from Goel et al. [32] and Mäkelä et al. [33] and was based on the decrease in phenolphthalein absorption after complexation with cyclodextrin. A working solution was prepared by mixing 20 mL of 125 mM $NaHCO_3$ with 800 µL ethanol and 200 µL of a 4 mM solution of phenolphthalein in ethanol. Centrifuged HPCD samples (14,000 rpm, RT, 20 min) were diluted with 50 mM TRIS/HCl pH 7.0 to an HPCD concentration of 0-100 µg mL^{-1}. The diluted samples (200 µL) were then mixed with 800 µL of working solution and the absorption at 550 nm was measured. For quantification, samples containing 0–50 µg mL^{-1} of HPCD were used for a calibration curve.

Software used and statistical analysis

Graphics shown in this work were generated using OriginPro 2023 (OriginLab Corporation, Northampton, USA) and GraphPad Prism 6 (GraphPad Software, Boston, USA). Molecular formulae shown in various figures were drawn using ChemDraw 22 (PerkinElmer Informatics, Waltham, USA). UPLC data were acquired and analysed using Empower 3 (Waters, Milford, USA). Time-dependent absorption measurements were analysed using LabSolutions UV-Vis software (Shimadzu Corporation, Kyoto, Japan). Fluorescence microscopic images were acquired, merged and edited using ZEN Microscopy software (Carl Zeiss, Oberkochen, Germany). Results of technical replicate experiments (n=2 or 3) are presented as mean±standard deviation.

Results

Initial setup for the whole-cell conversion of $VitD_3$ to 25OH$VitD_3$ by $S25DH_1$-producing *T. aromatica* resting cells

Using the recently established heterologous production platform for $S25DH_1$ in *T. aromatica* (*T. aromatica* pIZ1016_S25dCBAD), extracts from cells grown with benzoate and nitrate as carbon and energy sources converted 1 mM $VitD_3$ (0.385 g L^{-1}) to 25OH$VitD_3$ in ≈2 h with a yield of 90% [29]. In these assays, 10 mM $K_3[Fe(CN)_6]$ was used as electron acceptor. Here, we aimed to use this platform for the whole-cell conversion of $VitD_3$ to 25OH$VitD_3$ by coupling periplasmic $S25DH_1$ either to the endogenous respiratory chain of

T. aromatica via cytochrome c or to external electron acceptors. To control and optimise all relevant parameters, we opted for a resting cell approach in which precultured *T. aromatica* cells producing S25DH$_1$ were concentrated to a high-density suspension in a phosphate-buffered medium without supplements. In initial setups, *T. aromatica* was grown under denitrifying conditions in which benzoate was replaced by acetate. With continuously fed acetate and nitrate (molar 1:1 ratio), an optical density at 578 nm ($OD_{578\ nm}$) of 3–5 was achieved under nitrate limitation and permanent pH control; gene expression was induced by IPTG addition at $OD_{578\ nm} \approx 0.8$. Cells were washed with medium without acetate/nitrate, concentrated to $OD_{578\ nm} \approx 50$ (≈16 mg cell dry weight per mL corresponding to ≈8 mg protein per mL) and supplemented with 5% (w/v) HPCD and varying electron acceptors. The reaction was initiated by the addition of 0.5 mM VitD$_3$ and stopped with isopropanol, in which substrate and product were extracted.

The whole cell suspension converted VitD$_3$ to 25OHVitD$_3$ with the highest rates being observed in the presence of $K_3[Fe(CN)_6]$ (2 mM) or in air with an initial rate of about 0.2 nmol (mg protein)$^{-1}$ min^{-1} (Fig. 2A). When nitrate (2 mM) was used as acceptor under anoxic conditions, the conversion rate was only about 25%; the residual activity in the control without added electron acceptor can be attributed to residual endogenous electron acceptors. In a control experiment, isolated and enriched S25DH$_1$ did not use O_2 as direct electron acceptor, indicating that the observed O_2-dependent conversion in whole cells depends on the endogenous electron transfer chain including a terminal oxidase. The S25DH$_1$ activity per mg total protein in whole cells was approximately 60% of that in cell-free extracts (Fig. 2B). In contrast, cytoplasmic malate dehydrogenase activity was detected exclusively in cell-free extracts (Fig. 2C). This result indicates the integrity of the cells and excludes that S25DH$_1$ activity originates from extracts of lysed cells. In consistence with this finding, fluorescence microscopy showed that approximately 90% of cells used in the whole cell conversion of VitD$_3$ were viable (Fig. 2D).

We then tested the effect of the cell density on the VitD$_3$ conversion rate (Fig. S1). By incrementally increasing the $OD_{578\ nm}$ of the cell suspension from 10 to 50, an expected increase in the VitD$_3$ conversion rate was observed. A further doubling of $OD_{578\ nm}$ from 50 to 100 resulted only in a slight further increase of the overall VitD$_3$ conversion rate. Unless not otherwise stated, whole cell conversion experiments were henceforth performed with suspensions at $OD_{578\ nm} = 50$ (OD 50).

During whole-cell mediated VitD$_3$ bioconversion, ultra-performance liquid chromatography (UPLC) analysis of samples taken at different time points during the whole-cell VitD$_3$ conversion assays showed that 25OHVitD$_3$ is the only hydroxylated product, whereas not even traces of calcitriol or other trihydroxylated compounds were found (Fig. S2). Very minor peaks (maximum 1% within 24 h) are attributed to thermal/photochemical isomerisation products [34].

Optimized cultivation and stability of S25DH$_1$-producing *T. aromatica*

To optimise the growth yield of S25DH$_1$-producing *T. aromatica* cells, we tested different electron acceptors in combination with acetate as carbon and energy source. To ensure that the Moco biosynthetic machinery is upregulated [25, 29], nitrate was always added to the medium to serve either as an electron acceptor or

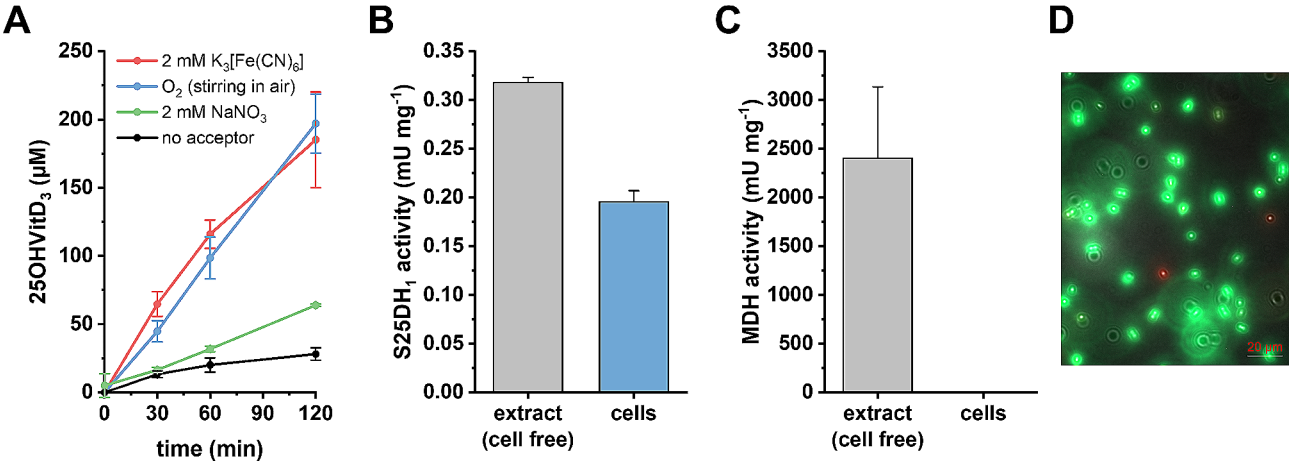

Fig. 2 Electron acceptor-dependent whole-cell conversion of 500 µM VitD$_3$ to 25OHVitD$_3$ by recombinant *T. aromatica* cells producing S25DH$_1$. (**A**), Electron acceptor dependence (0.25 mL scale, OD 50 corresponding to 4 mg cells [dry weight], 5% [w/v] HPCD, 1% [v/v] isopropanol). (**B**), S25DH$_1$ activity in cell free extracts and whole cells (0.1 mL scale, 0.1–0.3 mg total protein [whole cell or cell extract] 10% [w/v] HPCD, 1% [w/v] isopropanol, 10 mM $K_3[Fe(CN)_6]$); 1 mU refers to 1 nmol min^{-1}. (**C**), Malate dehydrogenase (MDH) activity in cell free extracts and whole cells; 1 mU refers to 1 nmol min^{-1}. (**D**), Fluorescence microscopy visualizing the ratio of living (green) and dead (red) cells

as the sole nitrogen source. Notably, S25DH$_1$ as well as the dissimilatory and assimilatory nitrate reductases all belong to the bis-molybdopterin dinucleotide cofactor-containing DMSO reductase enzyme family [25]. Therefore, the Moco biosynthetic machinery of S25DH$_1$ and nitrate reductases should be induced under the growth conditions used to ensure sufficient levels of the common cofactor [35].

Fully aerobic cultivation under continuous agitation in air resulted in maximum $OD_{578\ nm}$ values above 8 within 5 to 7 days, but the VitD$_3$ conversion rate in OD 50 cell suspensions dropped below 10% (Fig. S3) compared to OD 50 suspensions prepared from cells grown with acetate/nitrate. This finding is assigned to the reported oxygen sensitivity of S25DH$_1$ [25]. We therefore cultivated *T. aromatica* without stirring/shaking in aerobically prepared acetate/nitrate medium, referred to as semi-aerobic cultivation (Fig. 3A). In OD 50 suspensions of these cells, the conversion of VitD$_3$ was comparable to suspensions from cells anaerobically grown with acetate/nitrate. Notably, the conversion was significantly higher in resting than in exponentially growing cells, although the $OD_{578\ nm}$ of the resting cells decreased after two days of incubation at 30 °C. This finding suggests that there was an ongoing S25DH$_1$ synthesis in resting cells, and that S25DH$_1$ remained active under the semi-aerobic cultivation conditions. Indeed, the oxygen was readily consumed by *T aromatica* during the first 24 h, before a significant increase of $OD_{578\ nm}$ was observed (Fig. 3B). This observation is consistent with the finding that cells grown under denitrifying conditions use oxygen as a preferred electron acceptor during VitD$_3$ hydroxylation in

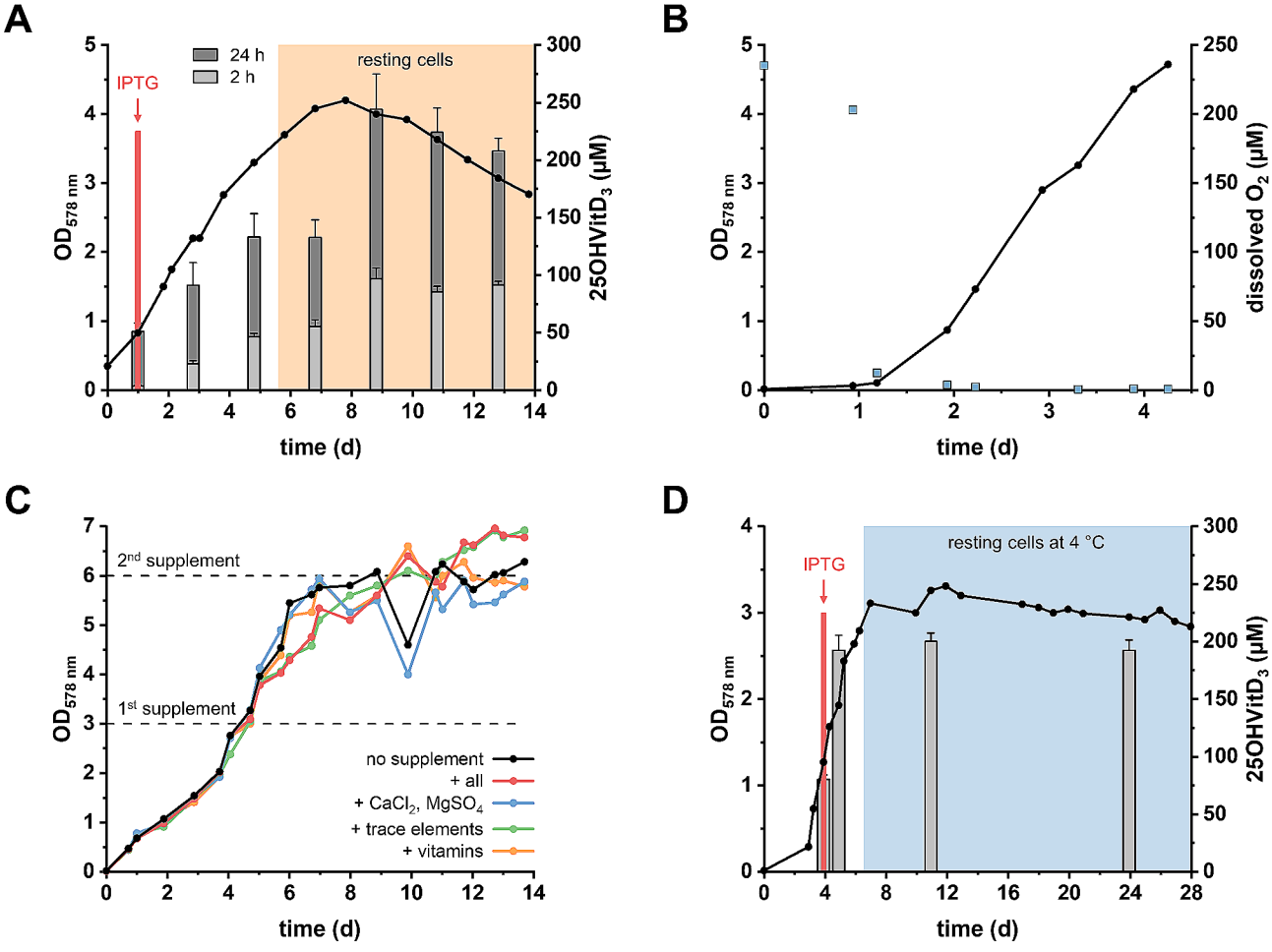

Fig. 3 Semi-aerobic cultivation of *T. aromatica* producing S25DH$_1$ with nitrate as electron acceptor. (**A**), Representative growth curve of *T. aromatica* producing S25DH$_1$ with acetate + nitrate (1:1) under aerobic conditions without stirring/shaking at 30 °C (semi-aerobic, black line), and formation of 25OHVitD$_3$ from 500 µM VitD$_3$ (grey bars) by cells taken at different time points (0.5 mL scale, OD 50 corresponding to 8 mg cells [dry weight], 5% [w/v] HPCD, 1% [v/v] isopropanol, aerobic). (**B**), Representative growth curve under semi-aerobic conditions (black line) and oxygen consumption (blue squares). (**C**), Growth curve to maximal $OD_{578\ nm}$ and the effect of supplementation as indicated by the horizontal dashed lines. (**D**), Stability of *T. aromatica* cells producing S25DH$_1$. Cells were grown under aerobic conditions + nitrate at 30 °C. After consumption of acetate/nitrate, the resting cells were stored at 4 °C; $OD_{578\ nm}$ (black line); 25OHVitD$_3$ formation within 2 h from 500 µM VitD$_3$ (grey bars) by cells taken at different time points (0.5 mL scale, OD 100 corresponding to 16 mg cells [dry weight], 5% [w/v] HPCD, 1% [v/v] isopropanol, aerobic)

T. aromatica cells and suggests that a terminal oxidase, most probably a low-affinity cytochrome cbb_3-type oxidase, is produced under denitrifying conditions [36]. In summary, oxygen removal by the endogenous aerobic respiratory chain was sufficient to maintain $S25DH_1$ activity if cells were not actively shaken or stirred. In further experiments to increase the maximal $OD_{578\ nm}$, different supplements were added. Indeed, supplementation with standard stock solutions of trace elements, vitamins or Ca^{2+}, Mg^{2+} [30] at $OD_{578\ nm}$ 3 resulted in a maximum $OD_{578\ nm}$ of 6.5. However, this value could not be further increased, neither by a second supplementation (Fig. 3C), nor by suspending washed cells in fresh medium.

At 30 °C, resting *T. aromatica* cells began to lyse after 2–3 days (Fig. 3A). Cell lysis was increased in dense suspensions above OD 10. At 4 °C, the OD of cells ($OD_{578\ nm}$ 3–4) and the $VitD_3$ conversion rate remained stable for up to three weeks under the previously defined semi-aerobic conditions (Fig. 3D). In conclusion, cell batches grown under semi-aerobic conditions were stored at 4 °C at $OD_{578\ nm} < 10$, which facilitated further optimisation of whole-cell $25OHVitD_3$ synthesis in identical cell batches.

Optimized solubilisation of $VitD_3$

Like other isoprenoid side-chain containing steroids, $VitD_3$ is almost insoluble in aqueous solutions. To overcome this problem in biocatalytic conversions of $VitD_3$, HPCD has often been used to increase its solubility by several orders of magnitude up to the millimolar range [37]. In addition, HPCD promotes the isomerization of $VitD_3$ to $preVitD_3$, which is proposed to be the actual substrate for $S25DH_1$ [28, 38].

The dependence of whole-cell conversions of $VitD_3$ to $25OHVitD_3$ on HPCD concentration was tested. In initial experiments, $VitD_3$ stock solutions were prepared in isopropanol, from which aliquots were transferred to the medium resulting in a maximum of 0.5 mM dissolved $VitD_3$ with 1% (v/v) isopropanol. In the absence of HPCD, virtually no formation of $25OHVitD_3$ from 0.5 mM $VitD_3$ was observed (Fig. 4A). The optimum HPCD concentration for the conversion of 0.5 mM $VitD_3$ was 5% (w/v), whereas at 7.5% (w/v), the conversion rate decreased. As reported for cell-free extracts [28], HPCD could not be substituted by organic solvents alone (isopropanol or ethanol, 1–10% [v/v], each) and only to a minor extent (< 20% $VitD_3$ conversion compared to 5% [w/v] HPCD) by detergents (Tween 20, Triton X-100, or N,N-dimethyldodecylamine N-oxide, 0.2% each).

To maximise the amount of $VitD_3$ solubilised in HPCD and co-solvent during the whole-cell conversion, stock solutions of 50% (w/v) HPCD in water and $VitD_3$ solutions (20–200 mM) in either isopropanol or ethanol (1–10% [v/v]) were mixed at different ratios and the amount of solubilised $VitD_3$ was determined by UPLC analysis. Under optimised conditions, up to 10 mM $VitD_3$ were dissolved in the presence of 10% (v/v) ethanol and 25% (w/v) HPCD in aqueous buffer (Fig. 4B). These concentrated stock solutions were then used for whole cell suspension experiments. The activity of cells was not affected at final isopropanol/ethanol concentrations of up to 5% (v/v) in the reaction buffer. However, no $VitD_3$ conversion was observed when HPCD was omitted in the presence of 5% (v/v) ethanol or isopropanol, respectively.

Whole-cell $25OHVitD_3$ synthesis under optimized and upscaled conditions

The optimised conditions for cell cultivation, $VitD_3$ solubilisation, and whole-cell conversion were applied to

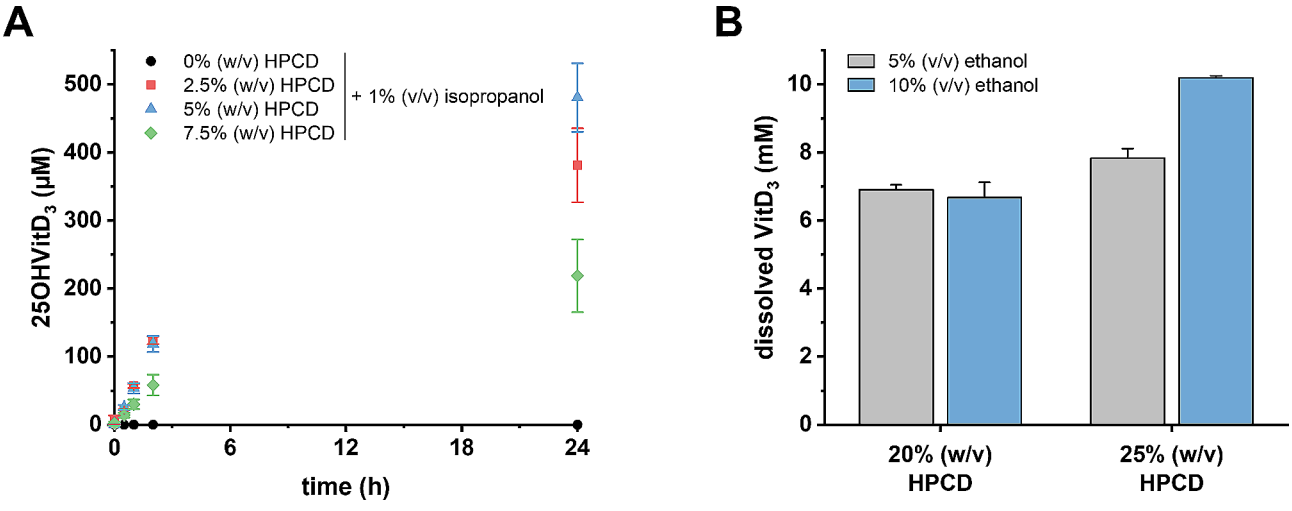

Fig. 4 Effect of HPCD and isopropanol on whole-cell conversion and solubilisation of $VitD_3$. (**A**), Effect of different HPCD concentrations on the formation of $25OHVitD_3$ from 500 µM $VitD_3$ (0.25 mL scale, OD 50 corresponding to 4 mg cells [dry weight], 1% [v/v] isopropanol, aerobic). (**B**), Experimentally determined $VitD_3$ concentrations in aqueous buffer using ethanol as co-solvent and HPCD

maximise biocatalytic conversion of $VitD_3$ to $25OHVitD_3$. In addition, we scaled up the volume from the typical 0.5 mL to the 100 mL scale. For this purpose, an OD 200 resting cell suspension was mixed with an aqueous solution containing ≈9.5 mM $VitD_3$, which was prepared in the presence of 25% (w/v) HPCD and 10% (v/v) ethanol as described above, resulting in a final concentration of 4.63 mM (1.78 g L^{-1}) $VitD_3$. To avoid inactivation of $S25DH_1$ due to oxygen exposure, we chose $K_3[Fe(CN)_6]$ as electron acceptor under anoxic conditions. In order to avoid conversion limitations due to electron acceptor consumption, $K_3[Fe(CN)_6]$ was added in 10 mM increments to a total concentration of 50 mM over the course of the 50 h incubation. Using this setup, a titer of ≈3.8 mM (1.52 g L^{-1}) $25OHVitD_3$ was achieved in the first 24 h, corresponding to 82% conversion. After prolonged incubation for further 26 h, the titer was increased to 1.85 g L^{-1} (4.6 mM) $25OHVitD_3$ corresponding to a >99% conversion (Fig. 5). Note that the apparent higher titer of the product compared to the substrate is due to the higher molecular weight.

Recycling of HPCD

The presence of HPCD is essential for an effective $VitD_3$ hydroxylation by whole-cell systems [37], and the high concentrations required significantly increase the overall cost of biocatalytic $25OHVitD_3$ synthesis. To overcome this limitation, we aimed to develop a recycling process for HPCD for its use in multiple cycles of $VitD_3$ bioconversion.

For HPCD recovery after $VitD_3$ conversion, cells were removed by centrifugation and unconverted $VitD_3$, the product $25OHVitD_3$ as well as the co-solvent isopropanol were extracted with ethyl acetate. The remaining aqueous phase contained HPCD and buffer components to which dH_2O was added to the initial volume after each cycle to compensate for the loss of medium during cell removal and ethyl acetate extraction (Fig. 6A). For the ten consecutive reaction cycles tested, fresh cell suspensions (OD 100) were used for each cycle. In control experiments, the identical cell suspension charge to which new medium with freshly prepared HPCD was used for each cycle. During each cycle, a loss of approximately 6–7% of HPCD was estimated in samples with recycled and with freshly added HPCD, due to sampling for HPCD analysis and centrifugation/extraction procedures in the laboratory scale. This loss was the same in samples with recycled or freshly added HPCD, indicating that HPCD was not degraded during the ten $VitD_3$ conversion cycles (Fig. 6B). The relative product formation was compared in samples with recycled vs. freshly added HPCD. Due to loss of HPCD after each cycle, a slight decrease of activity was expected in the samples using the recycled HPCD after each cycle. Although some variation was observed from cycle to cycle, the overall product formation indicates that recycled HPCD can replace freshly added HPCD (Fig. 6C). In conclusion, the established HPCD recycling process allows for multiple consecutive cycles of $VitD_3$ conversion.

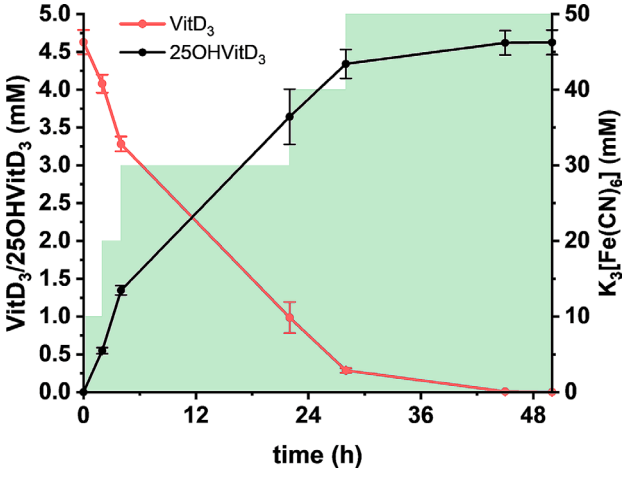

Fig. 5 Time course of optimised conversion of 4.63 mM $VitD_3$ to $25OHVitD_3$ using $S25DH_1$-producing resting *T. aromatica* cells (100 mL scale, OD 100 corresponding to 3.2 g cells [dry weight], 12.5% [w/v] HPCD, 5% [v/v] ethanol, 50 mM $K_3[Fe(CN)_6]$). Electron-accepting $K_3[Fe(CN)_6]$ was added in 10 mM increments (green shading)

Discussion

In this work, we have established a whole-cell system for the bioconversion of $VitD_3$ to $25OHVitD_3$ that has several advantages over conventional oxygenase-/peroxygenase-based systems with respect to the product titer, yield and selectivity. With 1.85 g $25OHVitD_3$ L^{-1}, the highest titer published was achieved with an almost complete conversion. Most importantly, the system hydroxylates $VitD_3$ in the desired C25-position with >>99% selectivity and does not produce even traces of the active hormone calcitriol.

The system using resting *T. aromatica* cells producing periplasmic $S25DH_1$ from *S. denitrificans* fulfils a number of mandatory requirements for an efficient whole-cell $25OHVitD_3$ synthesis (Fig. 7). Firstly, $VitD_3$ has to be taken up from the medium and transported across the outer membrane to reach periplasmic $S25DH_1$. This process is not trivial, as $VitD_3$ in the medium is tightly bound to HPCD forming a ≈2.85 kDa complex, from which it is unknown whether it can pass through an aqueous porin channel of the outer membrane from *T. aromatica*. However, considering that $preVitD_3$ rather than $VitD_3$ is the actual substrate of $S25DH_1$ [28], and that the equilibrium between both isomers is significantly shifted to $preVitD_3$ in the presence of HPCD [38], we assume that the $VitD_3$/HPCD complex does indeed pass the outer membrane. The transport of cyclodextrin across a porin has been demonstrated in a *Klebsiella* sp [39]. Regardless of whether $VitD_3$ in complex with HPCD

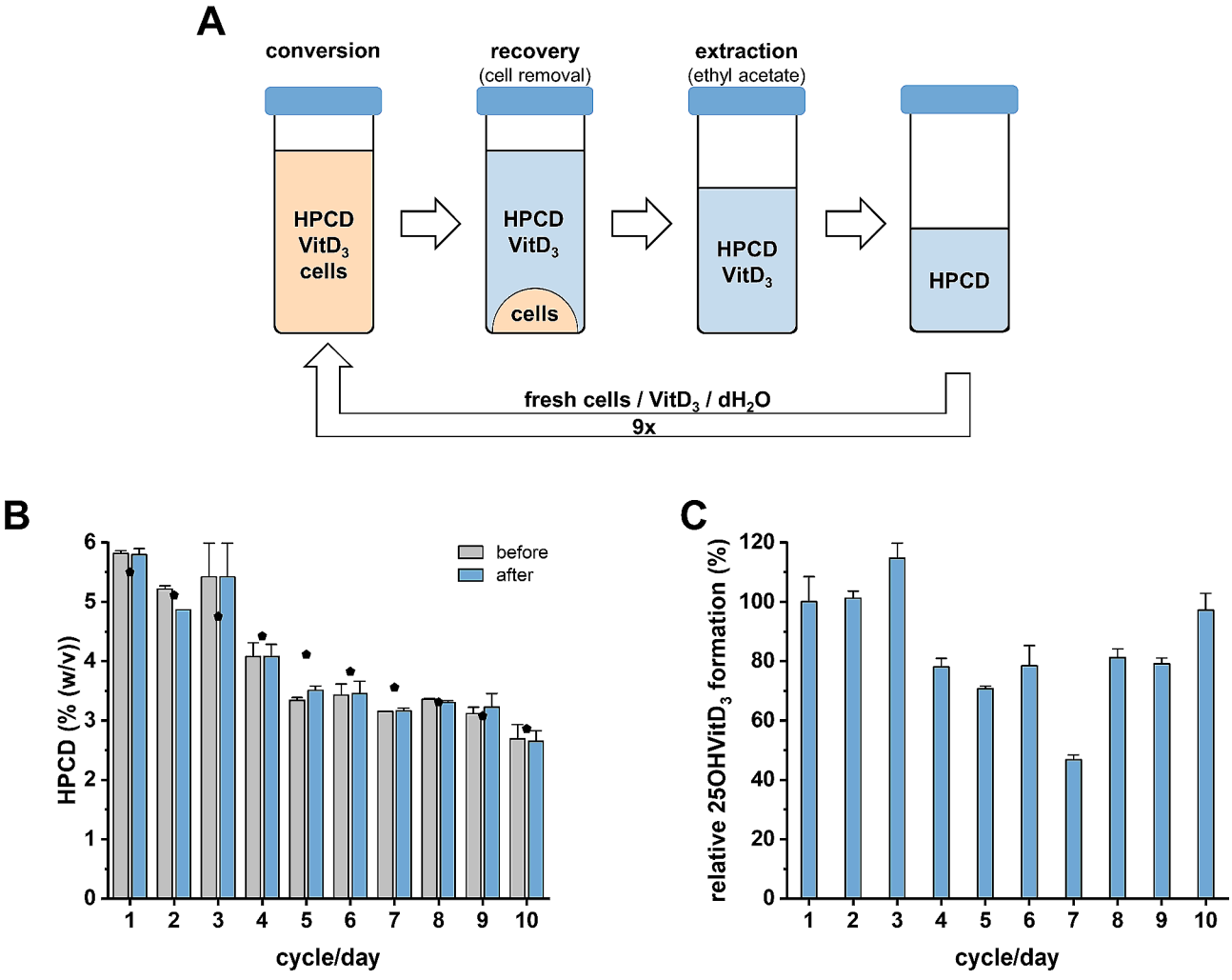

Fig. 6 HPCD recovery. (**A**), General recycling setup. (**B**), Experimentally determined HPCD concentrations before and after ten consecutive $VitD_3$ conversions. The black symbols represent the maximum expected HPCD concentration taking into account a 7% loss due to sampling and removal of cells and product. (**C**), Relative product formation in samples with freshly added HPCD (5% [w/v]) vs. recycled HPCD in ten consecutive $VitD_3$ conversions within 4 h (0.5 mL scale, OD 100 corresponding to 16 mg cells [dry weight], 1% [v/v] isopropanol, aerobic). 100% refer to the respective formation of $25OHVitD_3$ with freshly added HPCD in each cycle

passes the outer membrane, there will be an equilibrium between $preVitD_3$ and $VitD_3$ bound to cyclodextrin, to the outer and cytoplasmic membranes, and to the hydrophobic active site cavity of $S25DH_1$. In this context, it is important to offer an excess of HPCD in order to keep the vast majority of $VitD_3$/$25OHVitD_3$ in the medium. Once $VitD_3$ reaches the active site of $S25DH_1$, the hydroxylation of $VitD_3$ to $25OHVitD_3$ depends on an electron acceptor provided either by the endogenous O_2-/nitrate-dependent respiratory chains or by the artificial $K_3[Fe(CN)_6]$. Although O_2 and $K_3[Fe(CN)_6]$ gave comparable conversion rates under optimal agitation, the latter is preferred due to the oxygen sensitivity of $S25DH_1$. Oxygen damage to $S25DH_1$ becomes increasingly problematic when cells are used for multiple cycles. With nitrate, the conversion rate was significantly lower. It is noteworthy, that the $S25DH_1$ reaction generates electrons at a redox potential of the cytochrome c (>> +200 mV) rather than of quinone (+100 mV) level. Thus, a periplasmic nitrate reductase (NAP-type) could directly link $VitD_3$ hydroxylation to cytochrome c oxidation, probably in a rather unspecific manner. Such a scenario would explain the significantly lower rates with nitrate compared to O_2 or $K_3[Fe(CN)_6]$. NAP-type nitrate reductases can be induced in the stationary phase [40], which is in agreement with our observation that only resting but not exponentially growing cells accepted nitrate as an acceptor for $VitD_3$ hydroxylation. Irrespective of the acceptor used, it was important to use resting cells in the absence of an additional electron acceptor. This finding can be rationalised by a competition between $VitD_3$ and acetate (via its complete oxidation through the TCA

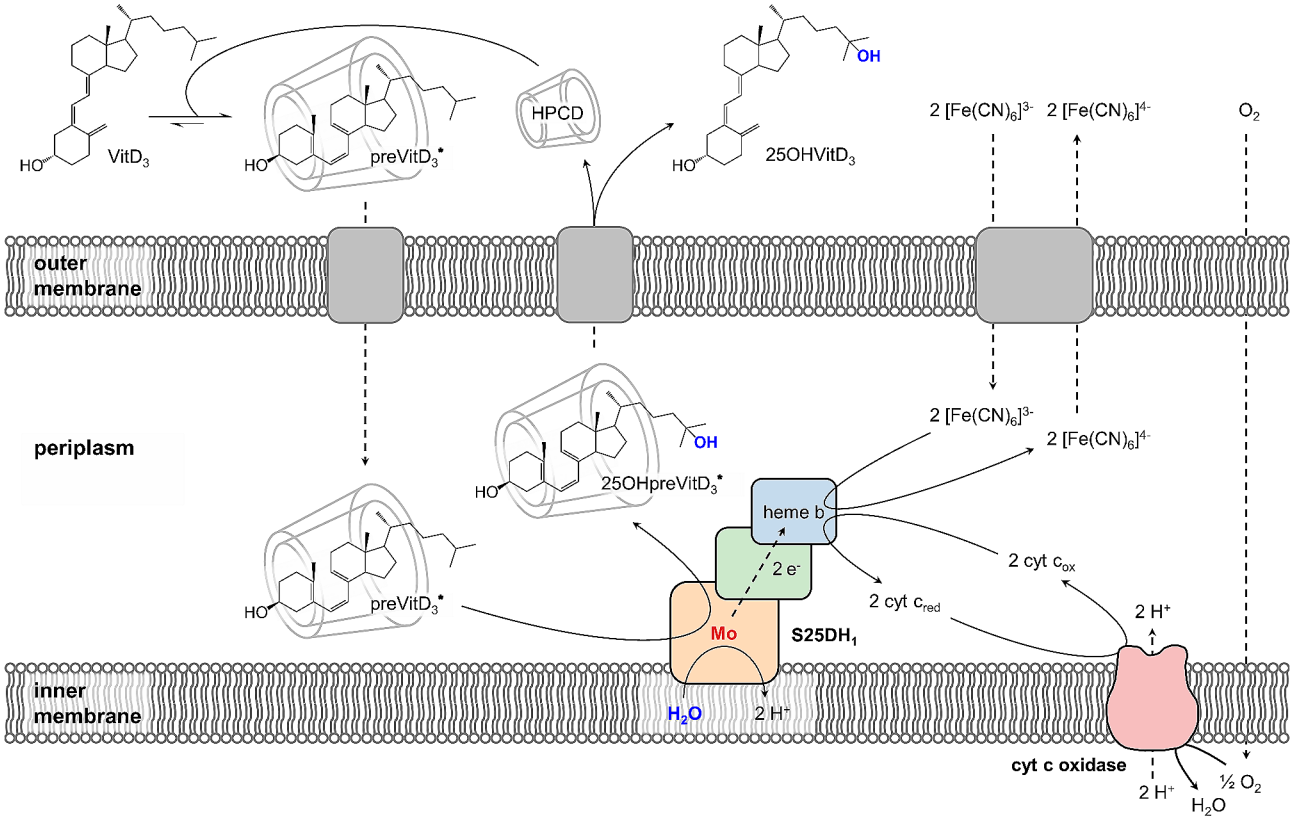

Fig. 7 Proposed model for the whole-cell synthesis of $VitD_3$ in $S25DH_1$-producing *T. aromatica*. The $preVitD_3$ form is favoured in the presence of HPCD and proposed to be the actual substrate of $S25DH_1$. It is unclear whether the $preVitD_3$/HPCD complex can pass the outer membrane through porins

cycle) as electron donors for $K_3[Fe(CN)_6]$ or O_2 reduction. After conversion, the hydroxylated product most likely crosses the outer membrane in the HPCD-bound state.

The workflow of the established whole-cell $25OHVitD_3$ synthesis system can be divided into three main steps: (i) cultivation of the biocatalyst, (ii) conversion of $VitD_3$ and (iii) processing of products and solvents (Fig. 8). Optimised cultivation was achieved under semi-aerobic conditions without stirring. Under these conditions, the O_2 concentration was sufficient to act as an acceptor but low enough to cause no significant inactivation of $S25DH_1$. Although we cannot exclude that some loss of $S25DH_1$ activity occurred, the semi-aerobic conditions turned out to be optimal to facilitate the overall bioconversion process. To stimulate the entire Moco biosynthetic machinery for the active site cofactor of $S25DH_1$, nitrate was always added to induce Moco-containing nitrate reductases [41]. It remains unclear why the growth of *T. aromatica* did not exceed $OD_{578\ nm}$ of 6.5 (semi-anaerobic) or 8 (aerobic), since even the exchange of medium did not allow higher cell densities to be achieved. On the other hand, the resting cells used for $VitD_3$ conversion were stable for weeks when kept at low temperatures. This finding allows the three steps of cultivation, conversion and processing to be carried out separately and continuously, which will be of great advantage for future applications.

In conclusion, despite the slower cultivation time of *T. aromatica* compared to established whole-cell systems (e.g. *E. coli*), the C25 dehydrogenase based system for the biocatalytic conversion of $VitD_3$ to $25OHVitD_3$ offers a number of advantages over previously reported biocatalytic systems. In order to scale up the process, a number of optimisations will need to be made in the future, in particular an increase in cell density and a better control of gene induction, ideally combined with the integration of the $S25DH_1$ genes into the genome under the control of an endogenous promoter.

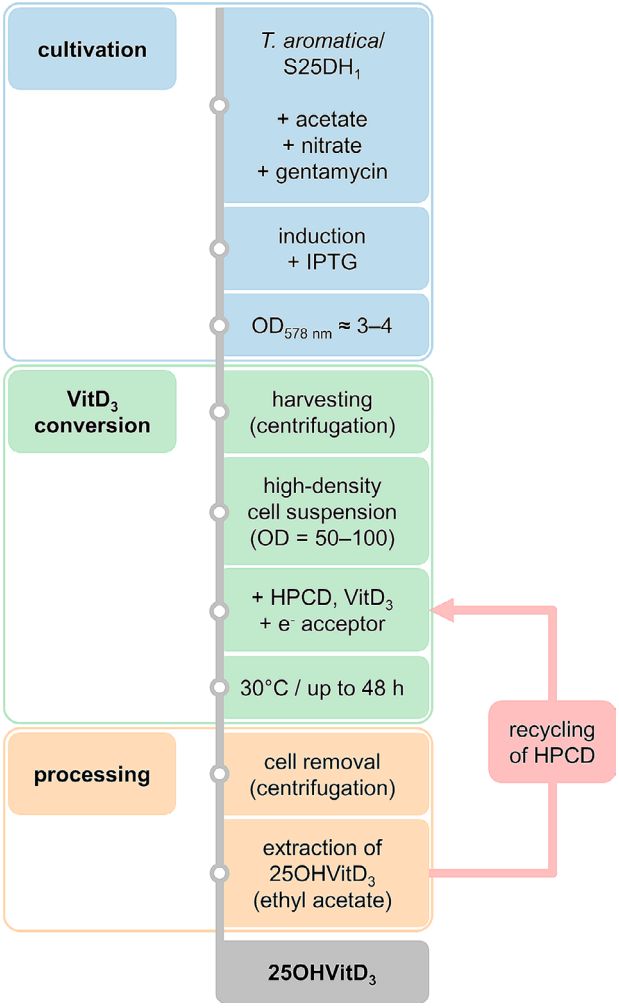

Fig. 8 Workflow for whole-cell 25OHVitD$_3$ biosynthesis using S25DH$_1$-producing *T. aromatica*

Abbreviations

CYP	Cytochrome P450
(d)dH$_2$O	(Double) distilled water
DMSO	Dimethylsulfoxid
$[Fe(CN)_6]^{3/4-}$	Ferricyanide
HPCD	2-hydroxypropyl-β-cyclodextrin
IPTG	Isopropyl β-D-1-thiogalactopyranoside
MDH	Malate dehydrogenase
Mo-*bis*PGD	Molybdo-*bis*-pyranopterin guanine dinucleotide
Moco	Molybdenum cofactor
NAP	Periplasmic nitrate reductase
$OD_{(578\ nm)}$	Optical density (at 578 nm)
25OHVitD$_{(3)}$	25-hydroxyvitamin D$_{(3)}$
S25DH$_{(1)}$	Steroid C25 dehydrogenase (isoform 1)
UPLC	Ultra-performance liquid chromatography
VitD$_{(2/3)}$	Vitamin D$_{(2/3)}$

Supplementary Information

The online version contains supplementary material available at https://doi.org/10.1186/s12934-024-02303-6.

Supplementary Material 1

Acknowledgements
We thank Christian Jacoby for providing the recombinant S25DH$_1$-producing *T. aromatica* cells that were used throughout this work, and Marleen Schultheis for evaluating different S25DH$_1$ gene expression systems.

Author contributions
M.W., O.M. and M.B. designed research; D.K., M.W., R.W. and C.E. performed research and analyzed data; D.K. designed and prepared the figures; D.K. and M.B. wrote the paper. All authors have given approval to the final version of the manuscript.

Funding
This work has been funded by the Koninklijke DSM N.V. (Kaiseraugst, Switzerland) and the German Federal Ministry of Education and Research (funding reference 031B1119A).
Open Access funding enabled and organized by Projekt DEAL.

Data availability
Data is provided within the manuscript or supplementary information file. Further data including source data are available from the corresponding author on reasonable request.

Declarations

Ethics approval and consent to participate
Not applicable.

Consent for publication
Not applicable.

Competing interests
The authors declare no competing interests.

Author details
[1]Faculty of Biology – Microbiology, University of Freiburg, 79104 Freiburg, Germany
[2]DSM Nutritional Products, Koninklijke DSM N.V., Kaiseraugst 4303, Switzerland

Received: 14 November 2023 / Accepted: 12 January 2024
Published online: 20 January 2024

References

1. Holick MF. The one-hundred-year anniversary of the Discovery of the Sunshine vitamin D3: historical, personal experience and evidence-based perspectives. Nutrients. 2023;15:593–615.
2. Holick MF. The vitamin D deficiency pandemic: approaches for diagnosis, treatment and prevention. Reviews in Endocrine and Metabolic Disorders. 2017;18:153–65.
3. Bouillon R, Marcocci C, Carmeliet G, Bikle D, White JH, Dawson-Hughes B, et al. Skeletal and extraskeletal actions of vitamin D: current evidence and outstanding questions. Endocr Rev. 2019;40:1109–51.
4. Rebelos E, Tentolouris N, Jude E. The Role of Vitamin D in Health and Disease: a narrative review on the mechanisms linking vitamin D with Disease and the effects of Supplementation. Drugs. 2023;83:665–85.
5. Abdrabbo M, Birch CM, Brandt M, Cicigoi KA, Coffey SJ, Dolan CC, et al. Vitamin D and COVID-19: a review on the role of vitamin D in preventing and reducing the severity of COVID-19 infection. Protein Sci. 2021;30:2206–20.
6. Charoenngam N, Shirvani A, Holick MF. Vitamin D and its potential benefit for the COVID-19 pandemic. Endocr Pract. 2021;27:484–93.
7. Jodar E, Campusano C, de Jongh RT, Holick MF. Calcifediol: a review of its pharmacological characteristics and clinical use in correcting vitamin D deficiency. Eur J Nutr. 2023;62:1579–97.
8. Bouillon R, Quesada Gomez JM. Comparison of calcifediol with vitamin D for prevention or cure of vitamin D deficiency. J Steroid Biochem Mol Biol. 2023;228:106248.
9. Quesada-Gomez JM, Bouillon R. Is calcifediol better than cholecalciferol for vitamin D supplementation? Osteoporos Int. 2018;29:1697–711.

10. Donati S, Marini F, Giusti F, Palmini G, Aurilia C, Falsetti I et al. Calcifediol: Why, When, How Much? Pharm 2023, Vol 16, Page 637. 2023;16:637–651.
11. Lütke-Dörhoff M, Schulz J, Westendarp H, Visscher C, Wilkens MR. Dietary supplementation of 25-hydroxycholecalciferol as an alternative to cholecalciferol in swine diets: a review. J Anim Physiol Anim Nutr (Berl). 2022;106:1288–305.
12. Soares JH, Kerr JM, Gray RW. 25-Hydroxycholecalciferol in Poultry Nutrition. 1995;74:1919–1934.
13. Vazquez JR, Gómez GV, López CC, Cortés AC, Díaz AC, Fernández SRT, et al. Effects of 25-hydroxycholecalciferol with two D3 vitamin levels on production and immunity parameters in broiler chickens. J Anim Physiol Anim Nutr (Berl). 2018;102:e493–7.
14. Zhu GD, Okamura WH. Synthesis of vitamin D (calciferol). Chem Rev. 1995;95:1877–952.
15. Turck D, Castenmiller J, De Henauw S, Hirsch-Ernst KI, Kearney J, Maciuk A, et al. Safety of calcidiol monohydrate produced by chemical synthesis as a novel food pursuant to regulation (EU) 2015/2283. EFSA J. 2021;19:e06660.
16. Wang Z, Zeng Y, Jia H, Yang N, Liu M, Jiang M, et al. Bioconversion of vitamin D3 to bioactive calcifediol and calcitriol as high-value compounds. Biotechnol Biofuels Bioprod. 2022;15:1–12.
17. Tang D, Liu W, Huang L, Cheng L, Xu Z. Efficient biotransformation of vitamin D3 to 25-hydroxyvitamin D3 by a newly isolated *Bacillus cereus* strain. Appl Microbiol Biotechnol. 2020;104:765–74.
18. Yasutake Y, Nishioka T, Imoto N, Tamura T. A single mutation at the ferredoxin binding site of P450 vdh enables efficient biocatalytic production of 25-hydroxyvitamin D3. ChemBioChem. 2013;14:2284–91.
19. Babot ED, del Río JC, Cañellas M, Sancho F, Lucas F, Guallar V, et al. Steroid hydroxylation by basidiomycete peroxygenases: a combined experimental and computational study. Appl Environ Microbiol. 2015;81:4130–42.
20. Li Y, Zhang P, Sun Z, Li H, Ge R, Sheng X, et al. Peroxygenase-catalyzed selective synthesis of Calcitriol starting from Alfacalcidol. Antioxidants. 2022;11:1044.
21. Fu B, Ren Q, Ma J, Chen Q, Zhang Q, Yu P. Enhancing the production of physiologically active vitamin D3 by engineering the hydroxylase CYP105A1 and the electron transport chain. World J Microbiol Biotechnol. 2022;38:1–10.
22. Schmitz LM, Kinner A, Althoff K, Rosenthal K, Lütz S. Investigation of Vitamin D2 and Vitamin D3 Hydroxylation by *Kutzneria albida* ChemBioChem. 2021;22:2266–74.
23. Abdulmughni A, Erichsen B, Hensel J, Hannemann F, Bernhardt R. Improvement of the 25-hydroxyvitamin D3 production in a CYP109A2-expressing *Bacillus megaterium* system. J Biotechnol. 2021;325:355–9.
24. Kang DJ, Im JH, Kang JH, Kim KH. Bioconversion of vitamin D3 to calcifediol by using resting cells of *Pseudonocardia* Sp. Biotechnol Lett. 2015;37:1895–904.
25. Dermer J, Fuchs G. Molybdoenzyme that catalyzes the anaerobic hydroxylation of a tertiary carbon atom in the side chain of cholesterol. J Biol Chem. 2012;287:36905–16.
26. Warnke M, Jacoby C, Jung T, Agne M, Mergelsberg M, Starke R, et al. A patchwork pathway for oxygenase-independent degradation of side chain containing steroids. Environ Microbiol. 2017;19:4684–99.
27. Rugor A, Wójcik-Augustyn A, Niedzialkowska E, Mordalski S, Staroń J, Bojarski A, et al. Reaction mechanism of sterol hydroxylation by steroid C25 dehydrogenase – homology model, reactivity and isoenzymatic diversity. J Inorg Biochem. 2017;173:28–43.
28. Warnke M, Jung T, Dermer J, Hipp K, Jehmlich N, von Bergen M, et al. 25-Hydroxyvitamin D 3 synthesis by enzymatic steroid side-chain hydroxylation with Water. Angew Chemie Int Ed. 2016;55:1881–4.
29. Jacoby C, Eipper J, Warnke M, Tiedt O, Mergelsberg M, Stärk H-J et al. Four Molybdenum-Dependent Steroid C-25 hydroxylases: Heterologous Overproduction, Role in Steroid Degradation, and application for 25-Hydroxyvitamin D 3 synthesis. MBio. 2018;9.
30. Anders HJ, Kaetzke A, Kampfer P, Ludwig W, Fuchs G. Taxonomic position of aromatic-degrading denitrifying pseudomonad strains K 172 and KB 740 and their description as new members of the genera *Thauera*, as *Thauera aromatica* sp. nov., and *Azoarcus*, as *Azoarcus evansii* sp. nov., respectively, members of the beta subclass of the Proteobacteria. Int J Syst Bacteriol. 1995;45:327–33.
31. Bradford MM. A rapid and sensitive method for the quantitation of microgram quantities of protein utilizing the principle of protein-dye binding. Anal Biochem. 1976;72:248–54.
32. Goel A, Nene SN. Modifications in the Phenolphthalein Method for Spectrophotometric Estimation of Beta Cyclodextrin. Starch - Stärke. 1995;47:399–400.
33. Mäkelä M, Korpela T, Laakso S. Colorimetric determination of β-cyclodextrin: two assay modifications based on molecular complexation of phenolphatalein. J Biochem Biophys Methods. 1987;14:85–92.
34. Woollard DC, Indyk HE, Gill BD. Significance of previtamin D chromatographic resolution in the accurate determination of vitamin D3 by HPLC–UV. J Food Compos Anal. 2019;79:1–4.
35. Zupok A, Iobbi-Nivol C, Mé V, Leimkü S. The regulation of Moco biosynthesis and molybdoenzyme gene expression by molybdenum and iron in bacteria. 1602 | Met. 2019;11:1602.
36. Kučera I, Sedláček V. Involvement of the cbb3-Type terminal oxidase in growth competition of Bacteria, Biofilm formation, and in switching between Denitrification and aerobic respiration. Microorganisms. 2020;8:1–11.
37. Wang F, Yu W, Popescu C, Ibrahim AA, Yu D, Pearson R, et al. Cholecalciferol complexation with hydroxypropyl-β-cyclodextrin (HPBCD) and its molecular dynamics simulation. Pharm Dev Technol. 2022;27:389–98.
38. Tian XQ, Holick MF. Catalyzed thermal isomerization between previtamin D3 and vitamin D3 via β-cyclodextrin complexation. J Biol Chem. 1995;270:8706–11.
39. Pajatsch M, Andersen C, Mathes A, Böck A, Benz R, Engelhardt H. Properties of a cyclodextrin-specific, unusual porin from *Klebsiella oxytoca*. J Biol Chem. 1999;274:25159–66.
40. Siddiqui RA, Warnecke-Eberz U, Hengsberger A, Schneider B, Kostka S, Friedrich B. Structure and function of a periplasmic nitrate reductase in *Alcaligenes eutrophus* H16. J Bacteriol. 1993;175:5867–76.
41. Luque-Almagro VM, Gates AJ, Moreno-Vivián C, Ferguson SJ, Richardson DJ, Roldán MD. Bacterial nitrate assimilation: gene distribution and regulation. Biochem Soc Trans. 2011;39:1838–43.

Publisher's Note